American Journal of Nanomaterials, 2019, Vol. 7, No. 1, 39-45
Available online at http://pubs.sciepub.com/ajn/7/1/5
Published by Science and Education Publishing
DOI:10.12691/ajn-7-1-5

Sol-gel Preparation of Different Crystalline Phases of TiO_2 Nanoparticles for Photocatalytic Degradation of Methylene Blue in Aqueous Solution

Siti Lailatul N. Zulmajdi[1], Nur Izzah I. Zamri[1], Abdul Hanif Mahadi[2], Mohd Yameany H. Rosli[3], Fairuzeta Ja'afar[1], Hartini M. Yasin[1], Eny Kusrini[4], Jonathan Hobley[1,5], Anwar Usman[1,*]

[1]Department of Chemistry, Faculty of Science, Universiti Brunei Darussalam, Jalan Tungku Link, Gadong BE1410, Brunei Darussalam
[2]Centre for Advanced Material and Energy Sciences, Universiti Brunei Darussalam, Jalan Tungku Link, Gadong BE1410, Negara Brunei Darussalam
[3]Physical & Geological Science Department, Universiti Brunei Darussalam, Jalan Tungku Link, Gadong BE1410, Negara Brunei Darussalam
[4]Department of Chemical Engineering, Faculty of Engineering, Universitas Indonesia, Kampus Baru UI, Depok 16424, Indonesia
[5]Current Address; OndaLabs, Mabalacat, Clark Freeport, Angeles, Pampanga, Philippines
*Corresponding author: anwar.usman@ubd.edu.bn

Received July 22, 2019; Revised August 28, 2019; Accepted September 09, 2019

Abstract This paper describes the photocatalytic degradation of methylene blue (MB) in aqueous solution in the presence of TiO_2 nanoparticles (NPs) in different compositions of anatase and rutile phases under UV light irradiation. The different compositions of crystalline phases of TiO_2 NPs were synthesized using sol-gel method at the same temperature for various calcination times. The TiO_2 NPs were subjected to crystal phase, vibrational, size, and morphological characterizations. The photocatalytic degradation of MB revealed that anatase TiO_2 NPs have a superior catalytic activity in the front of rutile phase. This finding further suggested that low charge resistance and low electron-hole recombination probability lead to the acceleration of the OH• formation on the surface of anatase TiO_2 NPs.

Keywords: *photocatalysis; titania; sol-gel; calcination time; methylene blue*

Cite This Article: Siti Lailatul N. Zulmajdi, Nur Izzah I. Zamri, Abdul Hanif Mahadi, Mohd Yameany H. Rosli, Fairuzeta Ja'afar, Hartini M. Yasin, Eny Kusrini, Jonathan Hobley, and Anwar Usman, "Sol-gel Preparation of Different Crystalline Phases of TiO_2 Nanoparticles for Photocatalytic Degradation of Methylene Blue in Aqueous Solution." *American Journal of Nanomaterials*, vol. 7, no. 1 (2019): 39-45. doi: 10.12691/ajn-7-1-5.

1. Introduction

Environmental problems related to chemical pollutants originating from the textile, leather, paper, rubber, plastics, cosmetic, commercial food, and pharmaceutical industries have become a serious global issue [1,2]. For instance, numerous types of industrial wastes containing synthetic dyes, heavy metals, fertilizers, and pesticides are discharged into water streams or sewage systems, and have caused severe problems such as eutrophication, perturbations in aquatic life, obstruction of marine plant photosynthesis, which affects the entire ecosystem. Amongst all of the pollutive chemicals, synthetic dyes from the textile industry can be very toxic and carcinogenic, even at low concentrations [2]. Therefore, effective techniques to remove synthetic dyes from industrial wastes prior to their discharge into sewage systems, water recycling systems, and water streams are vital to minimize the impact on the environment.

There have been countless reports focused on the development on the treatment of wastewater and remediation techniques, generally based on physical, chemical or biological methods, such as coagulation/flocculation and filtration [3], reverse osmosis membranes [4], advanced oxidation processes [5], adsorption [6,7], and microbial degradation [8,9] to eliminate, adsorb, or degrade synthetic dyes and other toxic chemical pollutants present in wastewater. Irrespective of the advantages and limitations of the proposed methods, photocatalytic degradation of dyes via their chemical reactions with generated hydroxyl (OH•) radicals at or near the surfaces of semiconductors has received much attention [10]. This is because photocatalytic degradation can completely degrade dyes under solar, UV, or visible light irradiation. Metal oxide semiconductors have been extensively used as a catalyst in photocatalytic degradation of dyes. Their band gap energy is in the UV or visible light region, thus, even sunlight could excite electrons from the valence band to the conduction band, making this method an inexpensive option [11-14].

Amongst many semiconductor nanomaterials, titanium dioxide nanoparticles (TiO_2 NPs) has been extensively investigated for environmental remediation applications [15-19]. The advantages of TiO_2 NPs as photocatalyst is supported by its chemical stability, distinct oxidation strength, low toxicity, low pollutant load, and availability at low-cost [20]. This topic has been reviewed in detail, for instance, by Tayeb and Hussein [2], Saeed et al. [21], and Pandey et al. [22]. The particle size has been proven to be the key factor of the photocatalytic activity of TiO_2 NPs [17]. Another important factor is the crystalline phase of TiO_2 NPs which can be attributed to phase-dependent Brunauer–Emmett–Teller (BET) surface area, pore size, and charge transfer resistance [18].

To explore the aforementioned issue, in this study, we investigated the photocatalytic activity of the different phases of TiO_2 NPs. We synthesized anatase and rutile TiO_2 NPs using sol-gel method, and utilized them as catalysts for the photodegradation of methylene blue (MB; 3,7-bis(dimethylamino)-phenothiazin-5-ium chloride) in aqueous medium, which can be considered as a model of wastewater contaminated by textile industries. The MB was selected as the pollutant because it is widely used as a reagent in redox titrations, a stain for surgical and medical marking, and a colorant in various industries. The morphology, percentage of elements, particle size, and crystalline phase of the synthesized TiO_2 NPs were determined by using scanning electron microscope (SEM), energy-dispersive X-ray spectroscopy (EDX), dynamic light scattering (DLS), and X-ray powder diffraction (XRD), respectively, while photodegradation of MB was monitored through the absorption of its solution using ultraviolet-visible (UV/VIS) spectrophotometer. The efficiency of the photocatalytic properties of the different phases of TiO_2 NPs and degradation kinetics of MB was also evaluated.

2. Experimental

2.1. Synthesis of TiO_2 NPs

TiO_2 NPs were synthesized using a wet method, namely sol-gel technique [23], with some modifications. First, 30 mL of 2-propanol (purchased from Sigma Aldrich) was mixed with 5 mL titanium(IV) tetraisopropoxide (TTIP) (purchased from Sigma Aldrich) with stirring for 0.5 hour at room temperature. Then 5 mL glacial acetic acid (purchased from Merck) at room temperature was added into the above clear mixture, forming the sol which was then kept at ambient temperature for 24 hours to ensure complete hydrolysis of the precursors. The obtained sol was then dispersed in distilled water, converting the sol to gel. The resulting cloudy suspension was then placed in an oven at 110 °C for 3 hours. The dried residue was calcined in a muffle furnace at 750°C at a heating rate of about 10 °C/min. The final product was then ground using mortar and pestle to give a fine, white powder. Depending on the calcination time, being 0.5, 1, 2, and 4 hours, the resulting TiO_2 NPs hereafter were abbreviated to be $TiO_2^{0.5}$, TiO_2^{1}, TiO_2^{2}, and TiO_2^{4}.

2.2. Material Characterizations

Crystalline phase of the resulting TiO_2 NPs were characterized using XRD on a Shimadzu X-ray diffractometer (XRD-7000) with Cu Kα radiation (λ = 0.15418 nm) reflection mode. XRD patterns were recorded over the 2θ range of 20–80°. The microscopic morphology of the TiO_2 NPs were obtained using a JEOL (JSM-7610F) scanning electron microscope (SEM) with 50000×magnification, and the elemental compositions were characterized using energy-dispersive X-ray (EDX) on AZtecOne (Oxford Instruments) spectroscope. Vibrational spectra of the TiO_2 NPs were recorded on a Shimadzu (IR Prestige-21) Fourier-transform infrared (FTIR) spectroscope (spectral range of 400-4000cm^{-1} with spectral resolution of 2.0 cm^{-1}) using potassium bromide (KBr) pellet method. The particle size of the TiO_2 NPs was evaluated by dynamic light scattering (DLS) measurement using a DLS (BI 9000, Brookhaven Instruments Corp) equipped with a 532 nm-diode laser.

2.3. Photocatalytic Reaction

Photocatalytic degradation of MB was carried out on a transparent glass reactor (7.5 cm diameter) containing the colloidal mixture of dispersed TiO_2 NPs and MB in aqueous solution. The colloidal mixture was stirred under darkness for 10 minutes to achieve adsorption-desorption equilibrium, and it was then irradiated with UV light emitting at 365 nm at different irradiation times of 0, 0.5, 1, 2, 3, 4, 5, 10, 15 and 30 minutes. During the irradiation, the colloidal mixture was continuously stirred, and excitation from the scattered UV and stray light were completely blocked. After irradiation at a certain desired time, the suspension was collected and separated by centrifugation at 3000 rpm for 15 minutes. The absorption spectrum of the supernatant was measured using Shimadzu (UV-1601PC) UV-visible spectrophotometer with a 1 cm quartz cuvette cell. The concentration of MB was determined by monitoring the changes in the absorbance maximum at 665 nm, at which it has an extinction coefficient of 7.4×10^4 L mol^{-1} cm^{-1}. To evaluate the effect of the initial MB concentration, it was varied to be in the range of 1.56–4.69×10^{-5} M, while the TiO_2 NPs was set at 5 mg L^{-1} and temperature was fixed at 25°C. From the effect of the initial MB concentration, we will elucidate the number of MB molecules per individual TiO_2 NPs to achieve optimum conditions for photocatalytic degradation. The effect of temperature of the photodegradation was elucidated by monitoring the photocatalytic degradation at different temperatures; 25, 30, 35, and 40 °C.

3. Results and Discussion

3.1. Morphological and Crystalline Phase Analysis

The morphology and structure of the synthesized TiO_2 NPs were characterized by SEM imaging, as shown in Figure 1. The SEM images indicate that all the

synthesized TiO_2 NPs are irregular to quasi-spherical in shape, with particle sizes of approximately 100 nm, similar to commercially available TiO_2 NPs. This was supported by the particle size determined using DLS, where all the synthesized and commercial anatase TiO_2 NPs are within 120±20 nm in diameter. The EDX data confirmed the formation of TiO_2. Overall, these results indicate that the sol-gel treatment, which occurs at ambient temperature and pressure, did not affect the morphology of TiO_2 NPs, nor did it induce the agglomeration of TiO_2 NPs. This further implies that all the synthesized TiO_2 NPs possess similar permeability, porous structure and surface area, and they are comparable with those of the commercial anatase, TiO_2^c NPs.

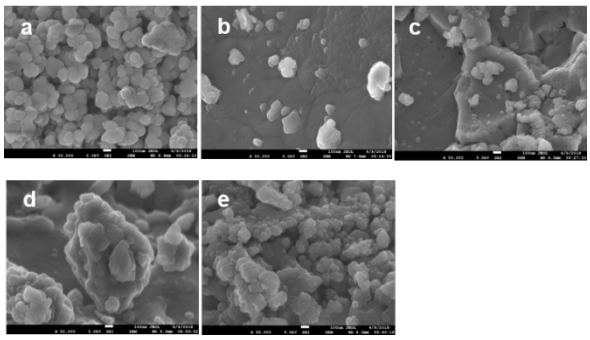

Figure 1. SEM images of TiO_2^c (a) along with $TiO_2^{0.5}$ (b), TiO_2^1 (c) TiO_2^2 (d), and TiO_2^4 (e). The scale bar in the images is of 100 nm

To determine the crystalline phases of the synthesized TiO_2 NPs, they were subjected to XRD measurement. As shown in Figure 2, the diffraction peaks of the TiO_2 NPs changes according to the different calcination times. The elongation of the calcination time from 0.5 to 4 hours resulted in the evolution of different diffraction peaks. A set of diffraction peaks appearing at 27.5, 36.1, 41,4, 44.2, 54.3, 56.7, and 69.2° are well indexed to the characteristic peaks of (110), (101), (111), (210), (211), (220), and (112) crystal planes of the rutile phase TiO_2 [24]. On the other hand, the set of peaks appear at 25.3, 37.7, 47.9, 53.9, 54.9, 62.6, and 68.9° can be well indexed to the characteristic peaks of (101), (004), (200), (105), (211), (204) and (116) crystal planes of anatase TiO_2 [24], and it is demonstrated for the TiO_2^c NPs. Based on the area of the diffraction peaks at 25.3° and 27.5°, which are the maximum characteristic peak for anatase and rutile phase, respectively, we estimated that the TiO_2 NPs has a mixture of anatase and rutile crystalline phases with the ratio 0.33:1, 0.25:1, 0.11:1, and 0.08:1 for $TiO_2^{0.5}$, TiO_2^1, TiO_2^2, and TiO_2^4, respectively, and the ratio was estimated to be 9:1 for the TiO_2^c NPs. The different ratios of the anatase and rutile crystalline phases can be expected to have different photocatalytic activities. Based on the diffraction peaks at 25.3° and 27.5°, we also estimated the crystallite size (D) of the TiO_2 NPs using the well-known Scherrer formula [25], $D = K \cdot \lambda/\beta \cos\theta$; (where K is the Scherrer constant, λ, the X-ray wavelength, β, the peak width of half maximum, and θ is the Bragg diffraction angle). The particle sizes of $TiO_2^{0.5}$, TiO_2^1, TiO_2^2, and TiO_2^4 NPs are in the range of 40.47–40.53 nm, whereas the estimated particle size of commercial anatase TiO_2 is 20.13 nm. These estimated values are much less than the actual particles sizes measured by using DLS, implying the limitation of the estimation on crystallite size based upon the XRD diffraction peak [26].

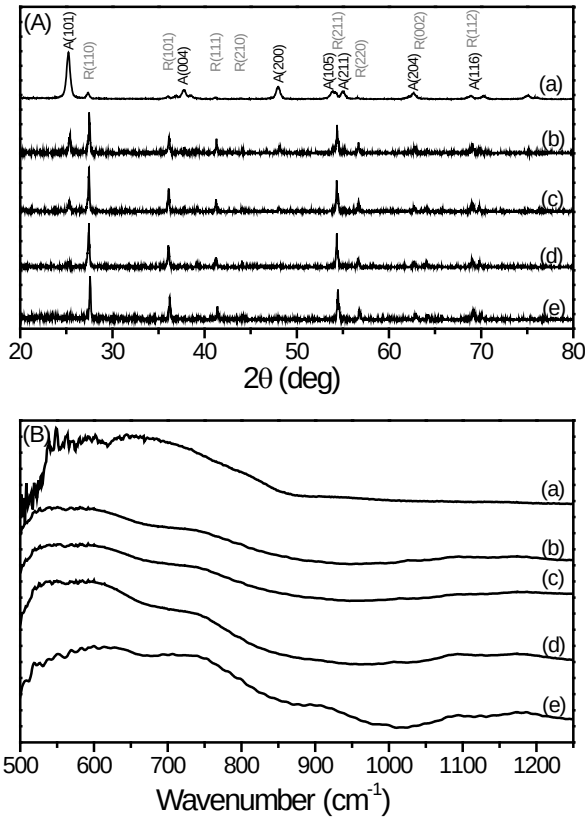

Figure 2. XRD pattern (A) and FTIR spectrum (B) of TiO_2^c (a), $TiO_2^{0.5}$ (b), TiO_2^1 (c), TiO_2^2 (d), and TiO_2^4 (e)

FTIR spectroscopy in the range of 500 to 1300 cm^{-1} was also used to characterize the series of synthesized TiO_2 NPs. As shown in Figure 3, the vibrational peak appears at 600 cm^{-1} due to the symmetric stretching vibrations of O–Ti–O in TiO_2, which is the determining peak for anatase TiO_2, and new vibrational bands at 738.8, 1087, and 1179 cm^{-1} were clearly observed with the development of the rutile phase. The FTIR spectrum of TiO_2^4, the highly rutile particles has an additional stretching at around 900 cm^{-1}. These new vibrational bands are most likely due to the anti-symmetric bending vibrations of O–Ti–O [27,28].

3.2. Photocatalytic Activity

The photocatalytic activities of different compositions of anatase/rutile TiO_2 NPs were evaluated on the basis of their ability to catalyze the degradation of MB under UV light irradiation. In the absence of TiO_2 NPs as catalyst, the photolysis of MB upon the UV irradiation was evaluated. The absorption peak of MB decreased gradually with irradiation time, where the peak intensity decreased by 0.11 OD which is approximately 10% after 30 min irradiation. This explains that even without the TiO_2 NPs, MB undergoes photolysis. With the same experimental conditions and irradiation time, the photocatalytic reactions for the degradation of MB in aqueous solution were then evaluated in the presence of the series of synthesized TiO_2 NPs as catalyst. Comparing with photolysis, the peak intensity decreased faster,

demonstrating the photocatalytic activity of the TiO_2 NPs. In the presence of the $TiO_2^{0.5}$ catalyst, complete degradation and decolorization took place within 3 hours, where the color of the colloidal mixture of dispersed TiO_2 NPs and MB in aqueous solution turned from blue to milky white.

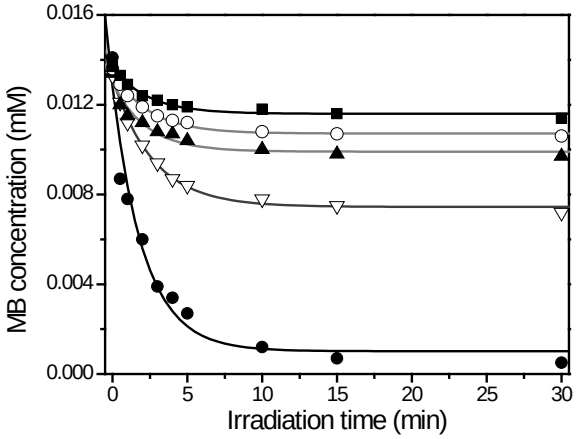

Figure 3. The degradation of MB concentration at different times of UV irradiation in the presence of TiO_2^c (●), $TiO_2^{0.5}$ (▽), TiO_2^1 (▲), TiO_2^2 (○), and TiO_2^4 (■) NPs catalysts. The lines are their respective best fitting with an exponential decay function

Figure 3 shows the degradation of MB concentration, which was calculated based on the absorbance and extinction coefficients, for different TiO_2 NPs as a function of irradiation time. Under the same experimental conditions, TiO_2^c NPs (anatase/rutile mixture 9:1) showed the strongest degradation of MB, implying the highest photocatalytic activity, followed by $TiO_2^{0.5}$, TiO_2^1, TiO_2^2, and TiO_2^4 NPs with anatase/rutile mixture of 0.33:1, 0.25:1, 0.11:1, and 0.08:1, respectively. This result suggested that the photocatalytic activity decreases with the reduction of anatase content in the mixture, implying that anatase TiO_2 NPs was more efficient for MB degradation, when compared to the rutile phase, as highlighted in literature [18,28]. Considering that the morphology, percentage of elements, and particle size should be the same for the anatase and rutile TiO_2 NPs [28,29]. These results clearly indicate that the different compositions of anatase/rutile mixture and the capability of TiO_2 NPs to adsorb MB on their surface are responsible for their distinct photocatalytic activity.

The photocatalytic reactions have been demonstrated and accepted to be pseudo-first order kinetics [30]. Therefore, the data of MB concentration as a function of irradiation time were fitted with a single-exponential decay function, $[MB] = [MB]_0 e^{-kt} + [MB]_{nd}$; (where $[MB]_t$, $[MB]_0$, and $[MB]_{nd}$ is the concentration at time t, the initial concentration, and the concentration of remaining MB after the irradiation, respectively). For the same initial MB concentration (1.56×10^{-5} M) and catalyst dosage (5 gL^{-1}), the photocatalytic degradation rate (k) of MB in the presence of different compositions of anatase/rutile TiO_2 mixture was estimated to be within 0.82-0.96 min^{-1}. However, the concentration of remaining MB after the irradiation was estimated to be 0.10, 0.75, 0.99, 1.07, and 1.16×10^{-5} M for TiO_2^c, $TiO_2^{0.5}$, TiO_2^1, TiO_2^2, and TiO_2^4 NPs, respectively. This implies that the photocatalytic efficiency was increased with the ratio of anatase/rutile TiO_2, revealing the distinctive photocatalytic activity of anatase TiO_2 NPs against its rutile phase. Similar results have been reported for the photocatalytic degradation of MB using UV and solar light [18,31,32]. It is noteworthy that the band gap energy of anatase and rutile phase is 3.21 and 3.00 eV, respectively, with similar absorbance at higher photon energy [33], implying that the different crystalline phases of TiO_2 should absorb similar number of photons from the 365-nm light excitation (3.39 eV). Thus, the effect of the excitation wavelength can be ruled out. The surface properties, particularly the orientation and coordination structure of surfaces of the different TiO_2 polymorph, which play a role in the adsorption and subsequent charge transfer to the dyes, can therefore be considered to contribute to the distinct photocatalytic activities of TiO_2 NPs. Therefore, the possible degradation process of MB should involve OH• free radical on the surface of TiO_2 NPs, when their electron gets excited from the valence to the conduction band under the UV light excitation and the electron in the conduction band reduces the dissolved oxygen [17,18,33]. Then, the OH• induces N-demethylation reaction of MB, leading to its degradation into H_2O, CO_2, and other organic molecules [34,35]. Considering that the electron conductivity, hole mobility, and the electron-hole recombination probability depend on the orientation and coordination structure of TiO_2 on the surface of the solid crystal, the higher photocatalytic activity of anatase TiO_2 NPs can be attributed to lower electron-hole recombination probability, leading to the acceleration of the OH• formation. In other words, the easy electron transport to the surface, rather than electron-hole recombination, contributes to the higher photonic efficiency of the anatase TiO_2 NPs, compared to the rutile phase. It is also worth mentioning that the shallow energy of the trap states in anatase TiO_2 NPs, in contrast to the deep energy of the trap states in rutile phase, has been demonstrated to have a contribution in its photocatalytic properties [36].

3.3. Effects of Dye Concentration and Catalyst Loading

The dye concentration plays a key role in the photocatalytic degradation. As shown in Figure 4(A), the effect of MB concentration (in the range of 1.56–4.69×10^{-5} M) on the photocatalysis of the dye in the presence of 5 mg L^{-1} of the synthesized TiO_2 NPs under UV light irradiation was investigated. The results demonstrated that the degradation rate increases with the initial MB concentration from 1.56 to 2.34×10^{-5} M, and it reduces at higher concentrations. Similar behavior was also observed for the commercial anatase TiO_2. This can be plausibly explained by considering that the amount of MB adsorbed on the surface of TiO_2 NPs increases with its initial concentration, resulting in higher efficient photocatalytic degradation. For the same number of TiO_2 NPs and irradiated photons, the OH• radicals formed on the surface of TiO_2 NPs is the same. In this condition, the photocatalytic degradation of MB increases with its initial concentration until it reaches a maximum.

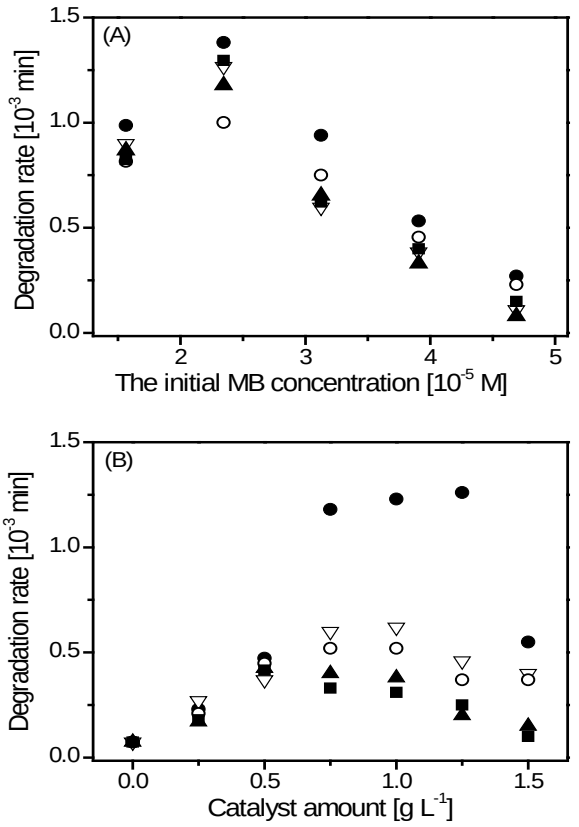

Figure 4. The effect of initial dye concentration (A) and catalyst dosage (B) on MB degradation in the presence of TiO_2^c (●), $TiO_2^{0.5}$ (▽), TiO_2^1 (▲), TiO_2^2 (○), and TiO_2^4 (■) NPs catalysts.

At the optimum condition, based on an effective molecular diameter of MB and the TiO_2 NPs with diameter of 100 nm, MB molecules adsorbed on the surface of individual TiO_2 NPs, irrespective of their crystalline phase, is roughly estimated to be 2.2×10^4, which is comparable to what has been previously reported [16]. At higher MB concentrations, the larger amounts of dye are adsorbed on the surface of TiO_2 NPs, hampering any direct contact of the dye with the OH• radicals. This so-called UV screening effect leads to an inhibitive effect on the dye degradation, thus the photocatalytic degradation rate becomes slower at higher MB concentrations. On the other hand, large amounts of the dye molecules do not have direct contact with TiO_2 NPs, nor with the generated OH• radicals, preventing them from successful photocatalytic degradation reactions and resulting in lower photonic efficiency. Thus, this suggests that larger catalyst surface area is required for the degradation of higher dye concentrations. Similar trends of concentration-dependent photocatalytic degradation of MB have been reported in literature [17,34,37,38].

To avoid the use of excess catalyst, as well as to further evaluate the ratio between the MB molecules and TiO_2 NPs in solution to achieve the optimum photocatalytic reaction, the catalyst loading TiO_2 NPs was varied from 0.25 to 25 mg L^{-1} at a constant MB concentration (1.56×10^{-5} M). As shown in Figure 4(B), the result demonstrated that the degradation rate of MB increases gradually in the case of 0.25 mg L^{-1} up to 1.25 mg L^{-1}, and it decreases sharply when the catalyst loading was above 1.5 mg L^{-1}. This finding has been explained on the basis that the optimum adsorption of the MB to react with the generated OH• radicals on the surface of TiO_2 NPs has been reached. When there is an excess of catalyst loading, the turbidity of the solution increases, causing elastic light scattering and shielding effect. This in turn decreases the incident UV light penetration, leading to the lower degradation rate of MB [13,39].

3.4. Effect of Temperature

Figure 5 shows the temperature dependence of the photocatalytic degradation rate of MB, where the degradation rate increases with temperature for all the different compositions of anatase/rutile TiO_2 NPs. By fitting the data points with linear Arrhenius equation, $\ln k = \ln A - E_a/RT$; (where A is the pre-exponential factor related to the frequency of successful degradation reaction, E_a is the activation energy, R is the universal gas constant (8.314 J K^{-1} mol^{-1}), and T is the absolute temperature), the activation energy related to the potential barrier of the photocatalytic degradation of MB was estimated from the slope of the respective curves to be 15.47, 20.84, 20.30, 20.74, and 19.40 kJ mol^{-1} for TiO_2^c, $TiO_2^{0.5}$, TiO_2^1, TiO_2^2, and TiO_2^4, respectively, which are comparable to reported in the literature [16,30,40,41]. This finding indicates that all the different compositions of anatase/rutile TiO_2 catalysts have a comparable capability to reduce the potential barrier of the photodegradation of MB. The comparable potential barrier of the different compositions of anatase/rutile TiO_2 catalysts is plausibly interpreted by considering that the photocatalytic oxidation of the MB dye on the surface of the TiO_2 NPs is controlled by the diffusion of the MB dyes and the generation of OH• radicals on the surface of TiO_2 NPs [2,13]. The OH• radicals is generated via the reduction of dissolved oxygen on the surface of the TiO_2 NPs by the electron in its conduction band. This means that the reduction and oxidation processes of the TiO_2 NPs depends on the photonic activation of the NPs. Therefore, the rate and the potential barrier of the photo-induced degradation of MB do not depend on the crystalline phase of TiO_2 NPs. However, the formation of OH• radicals on the surface of the TiO_2 NPs, which is responsible for the photocatalytic degradation, is governed by the orientation and coordination structure of TiO_2 on the surface of the solid crystal, thus the crystalline phase of TiO_2 NPs, as described in Section 3.2.

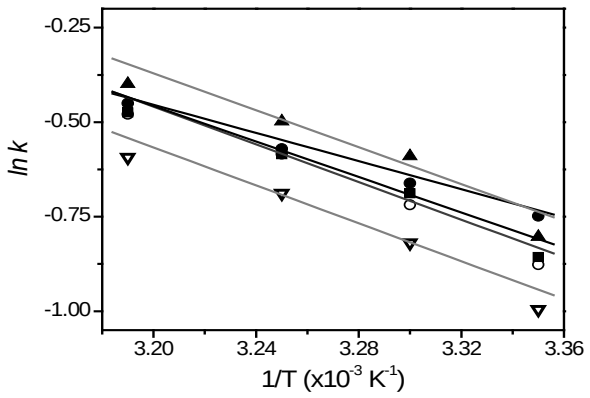

Figure 5. The plot of $ln\ k$ against inverse temperature, $1/T$, of the photocatalytic degradation of MB in the presence of TiO_2^c (●), $TiO_2^{0.5}$ (▽), TiO_2^1 (▲), TiO_2^2 (○), and TiO_2^4 (■) NPs catalysts. The straight lines are their respective best fit

4. Conclusion

In summary, the effect of the crystalline phase of TiO_2 nanoparticles on the photocatalytic activity of the degradation of methylene blue has been systematically investigated. The different crystalline phases of TiO_2 NPs with the comparable particle sizes were synthesized using the sol-gel method at 750°C for different calcination times in the range of 0.5–4 hours. The XRD diffraction results reveal the formation of different compositions of anatase and rutile phases of TiO_2 NPs. The photocatalytic degradation of methylene blue suggests that the anatase phase of TiO_2 NPs have better catalytic activity when compared to the rutile phase. This finding further suggested that low charge resistance and low electron-hole recombination probability lead to the acceleration of OH• formation on the surface of anatase TiO_2 NPs. The effect of temperature reveals that the different crystalline phases of TiO_2 NPs have a comparable capability to reduce the potential barrier of the photodegradation of MB. This suggested that the photocatalytic oxidation of the dye is controlled by the diffusion of the dyes and the generation of OH• radicals on the surface of TiO_2 NPs, rather than by the crystalline phase of the catalyst. The effect of the initial MB concentration provide the number of MB molecules per individual TiO_2 NPs to achieve optimum conditions for photocatalytic degradation.

Acknowledgements

The authors are grateful for the research facilities provided by Universiti Brunei Darussalam.

Conflict of Interest

The authors declare that they have no conflict of interest.

References

[1] Peleka, E.N. and Matis, K.A., "Water separation processes and sustainability," *Ind. Eng. Chem. Res.* 50, 421-430, 2011.

[2] Tayeb, A.M. and Hussein, D.S., "Synthesis of TiO2 nanoparticles and their photocatalytic activity for methylene blue," *Am. J. Nanomater.* 3, 57-63, 2015.

[3] Ma, B., Xue, W., Hu, C., Liu, H., Qu, J. and Li, L., "Characteristics of microplastic removal via coagulation and ultrafiltration during drinking water treatment," *Chem. Eng. J.* 359, 159-167, 2019.

[4] Tang, S.K., Teng, T.T., Alkarkhi, A.F.M. and Li, Z., "Sonocatalytic degradation of rhodamine B in aqueous solution in the presence of TiO_2 coated activated carbon," *APCBEE Proc.* 1, 110-115, 2012.

[5] Hisaindee, S., Meetani, M.A. and Rauf, M.A., "Application of LC-MS to the analysis of advanced oxidation process (AOP) degradation of dye products and reaction mechanisms," *Trends Anal. Chem.* 49, 31-44, 2013.

[6] Zaidi, N.A.H.M., Lim, L.B.L. and Usman, A., "Enhancing adsorption of malachite green dye using base-modified Artocarpus odoratissimus leaves as adsorbents," *Environ. Technol. Innovation* 13, 211-223, 2019.

[7] Kusrini, E., Wicaksono, W., Gunawan, C., Daud, N.Z.A. and Usman, A., "Kinetics, mechanism, and thermodynamics of lanthanum adsorption on pectin extracted from durian rind," *J. Environ. Chem. Eng.* 6, 6580-6588, 2018.

[8] Rubin, B.S. and Soto, A.M., "Bisphenol A: Perinatal exposure and body weight," *Molec. Cellular Endocrinol.* 304, 55-62, 2009.

[9] Hadibarata, T., Tachibana, S. and Askari, M., "Identification of metabolites from phenanthrene oxidation by phenoloxidases and dioxygenases of Polyporus sp. S133," *J. Microbiol. Biotechnol.* 21, 299-304, 2011.

[10] Ollis, D.F. and Al-Ekabi, H. (Eds.), "Photocatalytic Purification and Treatment of Water and Air," Elsevier, Amsterdam, 1993.

[11] Chakrabarti, S. and Dutta, B.K., "Photocatalytic degradation of model textile dyes in wastewater using ZnO as a semiconductor catalyst," *J. Hazard. Mater.* 112, 269-278, 2004.

[12] Behnajady M.A. and Eskandarloo, H., "Silver and copper co-impregnated onto TiO2-P25 nanoparticles and its photocatalytic activity," *Chem. Eng. J.* 228, 1207-1213, 2013.

[13] Jeni, J. and Kanmani, S., "Solar nanophotocatalytic decolorisation of reactive dyes using titanium dioxide," *Iran. J. Environ. Health. Sci. Eng.* 8, 15-24, 2011.

[14] Ratnawati, R., Gunlazuardi, J. and Slamet, S., "Development of titania nanotube arrays: The roles of water content and annealing atmosphere," *Mater. Chem. Phys.* 160, 111-118, 2015.

[15] Khataee, A.R. and Kasiri, M.B., "Photocatalytic degradation of organic dyes in the presence of nanostructured titanium dioxide: Influence of the chemical structure of dyes," *J. Mol. Catal. A Chem.* 328, 8-26, 2010.

[16] Zulmajdi, S.L.N., Ajak, S.N.F.H., Hobley, J., Duraman, N., Harunsani, M.H., Yasin, H.M., Nur, M. and Usman, A., "Kinetics of photocatalytic degradation of methylene blue in aqueous dispersions of TiO_2 nanoparticles under UV-LED irradiation," *Am. J. Nanomater.* 5, 1-6, 2017.

[17] Dariani, R.S., Esmaeili, A., Mortezaali, A. and Dehghanpour, S., "Photocatalytic reaction and degradation of methylene blue on TiO_2 nano-sized particles," *Optik* 127, 7143-7154, 2016.

[18] Prasannalakshmi, P. and Shanmugam, N., "Phase-dependant photochemistry of TiO_2 nanoparticles in the degradation of organic dye methylene blue under solar light irradiation," *Appl. Phys. A* 123, 586, 2017.

[19] Padovini, D.S.S., Magdalena, A.G., Capeli, R.G., Longo, E., Dalmaschio, C.J., Chiquito, A.J. and Pontes, F. M., "Synthesis and characterization of ZrO2@SiO2 core-shell nanostructure as nanocatalyst: Application for environmental remediation of rhodamine B dye aqueous solution," *Mater. Chem. Phys.* 233, 1-8, 2019.

[20] Wu, Y., Zhao, J., Li, Y. and Lu, K., "Preparation and freezing behavior of TiO_2 nanoparticle suspensions," *Ceram. Int.* 42, 15597-15602, 2016.

[21] Saeed, K., Khan, I., Gul, T. and Sadiq, M., "Efficient photodegradation of methyl violet dye using TiO_2/Pt and TiO_2/Pd photocatalysts," *Appl. Water Sci.* 7, 3841-3848, 2017.

[22] Pandey, A., Kalal, S., Ameta, C., Ameta, R., Kumar, S. and Punjabi, P.B., "Synthesis, characterization and application of naïve and nano-sized titanium dioxide as a photocatalyst for degradation of methylene blue," *J. Saudi Chem. Soc.* 19, 528-536, 2015.

[23] Cesnovar, A., Paunović, P., Grozdanov, A., Makreski, P. and Fidančevska, E., "Preparation of nano-crystalline TiO2 by sol-gel method using titanium tetraisopropoxide," *Adv. Nat. Sci.: Theory & Appl.* 1, 133-142, 2012.

[24] Sakurai K. and Mizusawa, M., "X-ray diffraction imaging of anatase and rutile," *Anal. Chem.* 82, 3519-3522, 2010.

[25] Kannadasan, N., Shanmugam, N., Cholan, S., Sathishkumar, K., Viruthagiri, G. and Poonguzhali, R., "The effect of Ce^{4+} incorporation on structural, morphological and photocatalytic characters of ZnO nanoparticles," *Mater. Charact.* 97, 37-46, 2014.

[26] Monshi, A., Foroughi, M.R. and Monshi, M.R., "Modified Scherrer equation to estimate more accurately nano-crystallite size using XRD," *World J. Nano Sci. Eng.* 2, 154-160 2012.

[27] Jo, W.-K. and Kim, J.-T., "Application of visible-light photocatalysis with nitrogen-doped or unmodified titanium dioxide for control of indoor-level volatile organic compounds," *J. Hazard. Mater.* 164, 360-366, 2009.

[28] Nolan, N.T., Seery, M.K. and Pillai, S.C., "Spectroscopic investigation of the anatase-to-rutile transformation of sol−gel-synthesized TiO_2 photocatalysts," *J. Phys. Chem.* 113, 16151-16157, 2009.

[29] Reyes–Coronado, D., Rodriguez–Gattorno, G., Espinosa–Pesqueira M.E., Cab, C., de Coss, R. and Oskam G., "Phase–pure TiO_2 nanoparticles: anatase, brookite, and rutile," *Nanotechnology* 19, 145605-145614, 2008.

[30] Salehi, M., Hashemipour, H. and Mirzaee, M., "Experimental study of influencing factors and kinetics in catalytic removal of methylene blue with TiO_2 nanopowder," *Am. J. Environ. Eng.* 2, 1-7, 2012.

[31] Andronic, L., Andrasi, D., Enesca, A., Visa, M. and Duta, A. "The influence of titanium dioxide phase composition on dyes photocatalysis," *J. Sol-Gel Sci. Technol.* 58, 201–208, 2011.

[32] Liu, L., Zhao, H., Andino, J.M. and Li, Y., "Photocatalytic CO_2 reduction with H_2O on TiO_2 nanocrystals," *ACS Catal.* 2, 1817-1828, 2012.

[33] Luttrell, T., Halpegamage, S., Tao, J., Kramer, A., Sutter, E. and Batzill, M., "Why is anatase a better photocatalyst than rutile?--Model studies on epitaxial TiO_2 films," *Sci. Rep.* 4, 40431-40438, 2015.

[34] Dai, K., Lu, L. and Dawson, G., "Development of UV-LED/TiO_2 device and their application for photocatalytic degradation of methylene blue," *J. Mater. Eng.Perform*. 22 1035-1040, 2013.

[35] Zhang, T.Y., Oyama, T., Aoshima, A., Hidaka, H., Zhao, J.C. and Serpone, N., "Photooxidative *N*-demethylation of methylene blue in aqueous TiO_2 dispersions under UV irradiation," *J. Photochem. Photobiol. A* 140, 163-172, 2001.

[36] Wang, X., Feng, Z., Shi, J., Jia, G., Shen, S., Zhou, J. and Li, C., "Trap states and carrier dynamics of TiO_2 studied by photoluminescence spectroscopy under weak excitation condition," *Phys. Chem. Chem. Phys.* 12, 7083-7090, 2010.

[37] Banat, F., Al-Asheh, S., Al-Rawashteh, M. and Nusair, M., "Photo-degradation of methylene blue dye bye the UV/H_2O_2 and UV/aceton oxidation processes," *J. Desalination.* 18, 225-232, 2005.

[38] Ling, C. and Mohamed, A., "Photo degradation of methylene blue dye in aqueous stream," *J. Technol.* 40, 91-103, 2004.

[39] Alkaim, A.F., Kandiel, T.A., Hussein, F.H., Dillert, R. and Bahnemann, D. W., "Solvent-free hydrothermal synthesis of anatase TiO_2 nanoparticles with enhanced photocatalytic hydrogen production activity," *Appl. Catal. A: General* 466, 32-37, 2013.

[40] Benetoli, L. O. de B., Cadorin, B. M., Postiglione, C. da S., de Souza, I.G., and Debacher, N.A., "Effect of temperature on methylene blue decolorization in aqueous medium in electrical discharge plasma reactor," *J. Braz. Chem. Soc.*, 22, 1669-1678, 2011.

[41] Lee, B.-N., Liaw, W.-D. and Lou, J.-C., "Photocatalytic Decolorization of Methylene Blue in Aqueous TiO2 Suspension," *Environ. Eng. Sci.* 16, 165-175, 1999.